



## Original articles

Research article

<https://doi.org/10.17308/kcmf.2024.26/12221>**Synthesis of nanoscale nickel (II) ferrite and a study of its catalytic and sorption activities towards methyl orange**A. A. Meshcheryakova<sup>1✉</sup>, E. V. Tomina<sup>1,2</sup>, S. A. Titov<sup>1</sup>, Nguyen Anh Tien<sup>3</sup>, A. I. Dmitrenkov<sup>2</sup><sup>1</sup>Voronezh State University,  
1 Universitetskaya pl., Voronezh 394018, Russian Federation<sup>2</sup>Voronezh State University of Forestry and Technologies named after G. F. Morozov  
8 Timiryazeva st., Voronezh 394087, Russian Federation<sup>3</sup>Ho Chi Minh City University of Education,  
280. An Duong Vuong st., District 4, District 5, Ho Chi Minh City, Vietnam**Abstract**

Nanoscale magnetic spinel ferrites are attracting an increased attention as functional materials for catalysis and sorption. Such catalysts and sorbents are advantageous due to their chemical stability in aggressive media, their thermal stability, a large area of specific surface, and high saturation magnetization, which allows using them to create magnetically controlled functional materials. This article presents the results of the synthesis of nickel (II) ferrite nanopowder, its characterization, and a study of its catalytic and sorption activities towards methyl orange dye.

X-ray diffraction (XRD), transmission electron microscopy (TEM), and scanning electron microscopy (SEM) were used to characterize nanocrystalline NiFe<sub>2</sub>O<sub>4</sub> synthesized by citrate combustion. The nickel spinel was tested as a catalyst of Fenton-like reaction of oxidative degradation of methyl orange under UV irradiation of  $\lambda = 270$  nm. The study involved differentiation of oxidation during dye sorption on a NiFe<sub>2</sub>O<sub>4</sub> nanoscale catalyst. The oxidative degradation of the pollutant under ultraviolet irradiation in the presence of a catalyst was satisfactorily described by a pseudo-first-order model, the rate constant of the reaction was 0.0191 min<sup>-1</sup>. The degree of methyl orange destruction reached 99% 150 minutes after the beginning of the reaction. A parallel experiment without the addition of hydrogen peroxide to the dye solution allowed assessing the sorption capacity of nanoscale nickel (II) ferrite. After 150 minutes, the concentration of the dye decreased by 7.5% due to its sorption, the equilibrium sorption capacity of NiFe<sub>2</sub>O<sub>4</sub> was low (0.132 mg/g). This indicates that the methyl orange solution decolorizes mainly due to its catalytic oxidative degradation according to the Fenton reaction.

This allows considering nanoscale nickel ferrite as a promising material for wastewater treatment by deep oxidation of organic pollutants.

**Keywords:** Nickel ferrite, Nanopowder, Photocatalysis, Fenton reaction**Funding:** The study was supported by Russian Science Foundation grant No. 23-23-00122, <https://rscf.ru/project/23-23-00122/>**Acknowledgements:** The research results were partially obtained using the equipment of the Center for Collective Use of Scientific Equipment of Voronezh State University. URL: <http://ckp.vsu.ru>.**For citation:** Meshcheryakova A. A., Tomina E. V., Titov S. A., Nguyen A. T., Dmitrenkov A. I. Synthesis of nanoscale nickel (II) ferrite and a study of its catalytic and sorption activities towards methyl orange. *Condensed Matter and Interphases*. 2024;26(3): 456–463. <https://doi.org/10.17308/kcmf.2024.26/12221>**Для цитирования:** Мещерякова А. А., Томина Е. В., Титов С. А., Нгуен А. Т., Дмитренко А. И. Синтез, исследование каталитической и сорбционной активности наноразмерного феррита никеля (II) в отношении метилового оранжевого. *Конденсированные среды и межфазные границы*. 2024;26(3): 456–463. <https://doi.org/10.17308/kcmf.2024.26/12221>✉ Anna A. Meshcheryakova, e-mail: [anna-meshcheryakova@internet.ru](mailto:anna-meshcheryakova@internet.ru)

© Meshcheryakova A. A., Tomina E. V., Titov S. A., Vo Kuang Mai, Nguen An' T'en, Dmitrenkov A. I., 2024



## Introduction

In recent years, there has been a growth of interest in nanoscale spinel ferrites as multifunctional materials. Using nanoscale spinels ( $\text{NiFe}_2\text{O}_4$  where  $\text{Me} = \text{Zn, Ni, Mg, Co, Mn}$ ) as catalysts and sorbents is advantageous due to their chemical stability in acid media, thermal stability, a highly developed surface, and high saturation magnetization [1, 2]. The magnetic properties of ferrites allow using them to create magnetically controlled functional materials, primarily catalysts and sorbents.

Currently, spinel ferrite-based catalysts have a wide range of applications, such as oxidative dehydration of hydrocarbons, decomposition of alcohols, and purification of exhaust gases generated by cars [3–6].

Spinel ferrites [7,8] and ferrite-based nanocomposites [9–11] are used in a number of technologies for wastewater treatment from pollutants: dyes, antibiotics, phenol derivatives, etc.

Nanoscale catalysts and sorbents should not only have high activity due to their developed surface with a large number of active sites, but also be products of energy-efficient and resource-saving technologies in order to economically justify their industrial implementation. For large-scale practical use of ferrites, it is necessary to distinguish simple, reproducible, and economical methods of their synthesis among the many known methods of synthesis [12–16]. These methods should allow regulating the characteristics of nanoscale spinel ferrites and obtaining samples with a large number of active sites for catalysis and sorption and magnetic properties necessary and sufficient to control the external magnetic field.

The purpose of this study was to synthesize nanoscale nickel (II) ferrite, a soft magnetic material with a reverse spinel structure, by citrate combustion and to test it as a catalyst for a Fenton-like reaction of oxidative degradation of the methyl orange dye.

## Experimental

$\text{NiFe}_2\text{O}_4$  synthesis was carried out by citrate combustion according to [17]. Phase composition was determined by X-ray diffractometry (Empyrean BV diffractometer with Cu anode ( $\lambda = 1.54060 \text{ nm}$ )). The scanning was performed

within a range of angles  $2\theta = 10\text{--}80^\circ$  with a step of 0.0200. The JCPDC database [18] was used to identify the phases (card 54-0964) [18]. The size and morphology of particles were determined by transmission electron microscopy (TEM, CarlZeiss Libra-120 transmission electron microscope). SEM image of the sample and quantitative elemental analysis was performed on a JSM-6380LV JEOL scanning electron microscope with an INCA 250 microanalysis system.

The catalytic activity of nanoscale nickel (II) ferrite was studied in a model reaction of methyl orange (MO) oxidation by hydrogen peroxide. To do this, we prepared a solution containing 0.0100 mg/ml of methyl orange and 10 wt. % of hydrogen peroxide. pH of the solution, which was 4.5, was maintained by an acetate buffer. Then, 0.2500 g of catalyst was added to a series of solution samples with a volume of 15.00 ml. Control measurements of the concentrations of MO solutions without a catalyst were performed in the same manner.

The experiment was conducted under ultraviolet irradiation with  $\lambda = 270 \text{ nm}$  (LightBest UV lamp, 25 W). The MO concentration was determined using photocolometry (KFK-3-01 photocolometer). The analytical wavelength for MO was 364 nm. The degree of degradation was calculated by formula (1):

$$W = \frac{C_0 - C_t}{C_0} \cdot 100 \%, \quad (1)$$

where  $W$  is the degree of degradation %,  $C_0$  is the concentration of the dye at the initial moment of time, and  $C_t$  is the concentration of the dye at the present moment of time.

To differentiate the catalytic oxidation and sorption of the dye on a nanoscale  $\text{NiFe}_2\text{O}_4$  catalyst, we performed an experiment using the above-described method in the darkness without adding  $\text{H}_2\text{O}_2$  oxidant to the solutions. In this case, oxidative degradation of MO was not performed, while decolorization of the solution was only determined by the sorption of the pollutant on ferrite. The duration of static sorption was 2 hours. The sorption capacity of nickel ferrite (II) was determined using equation (2):

$$A = \frac{(C_0 - C) \cdot V}{m}, \quad (2)$$

where  $C_0$  is the initial concentration of the solution of the organic dye, mol/l;  $C$  is the concentration of the organic dye after a certain time after the beginning of the reaction, mol/l;  $V$  is the volume of the adsorbate solution, l;  $m$  is the weight of ferrite, g.

**Results and discussion**

Reflexes in the diffraction patterns of the nanopowder synthesized by citrate combustion (Fig. 1) referred to the target phase of  $NiFe_2O_4$  (JCPDC 54-0964). We also identified a single low-intensity reflex of  $Fe_2O_3$  iron oxide, however, it did not seem critical due to the potential catalytic activity of the  $Fe^{3+}$  ion.

The average size of coherent scattering regions (CSRs) of  $NiFe_2O_4$  particles calculated using the Debye–Scherrer formula [19] was  $31 \pm 2$  nm.

TEM (Fig. 2.) showed that the shape of  $NiFe_2O_4$  particles was close to spherical. There

were individual coarse particles with a size of 90–100 nm, however, the predominant particle size fraction was in the range of 21–50 nm. According to TEM data, the average size of  $NiFe_2O_4$  particles was  $38 \pm 3$  nm. According to XRD, the calculated CSR values generally correlated with the TEM results.

The average values of the weight and atomic percentages of the Ni, Fe, and O elements according to the data of energy dispersion analysis (Table 1) correlate with the expected chemical composition of the synthesized samples. The presence of residual carbon on the energy dispersive spectrum (Fig. 3) indicated the probable accumulation of solid x-ray amorphous products of gel degradation in the pores of the nanopowder without complete oxidation of the combustion products.

The surface of nickel (II) ferrite was characterized by a “coral-like” structure,

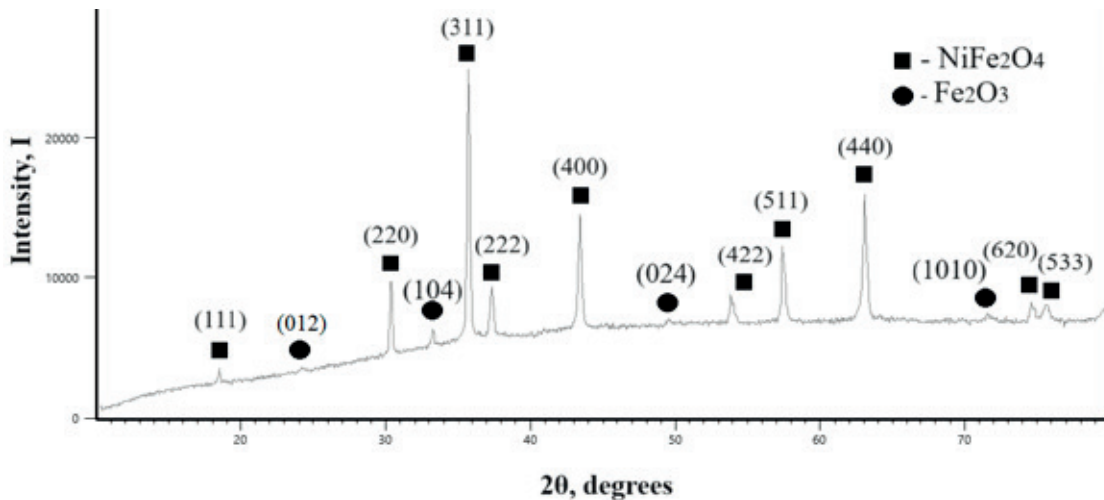


Fig. 1. Diffraction pattern of  $NiFe_2O_4$  nanopowder

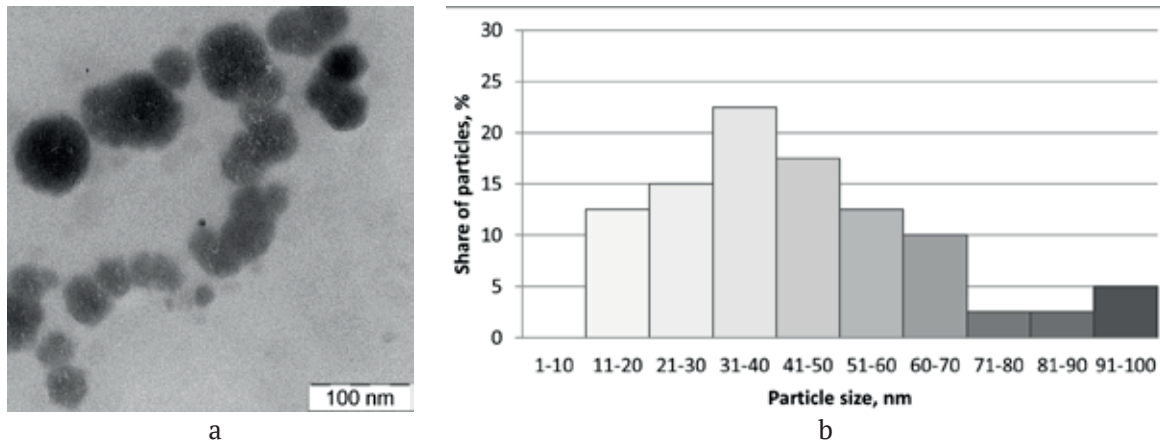


Fig. 2. TEM image (a) and histogram of  $NiFe_2O_4$  particle size distribution (b)

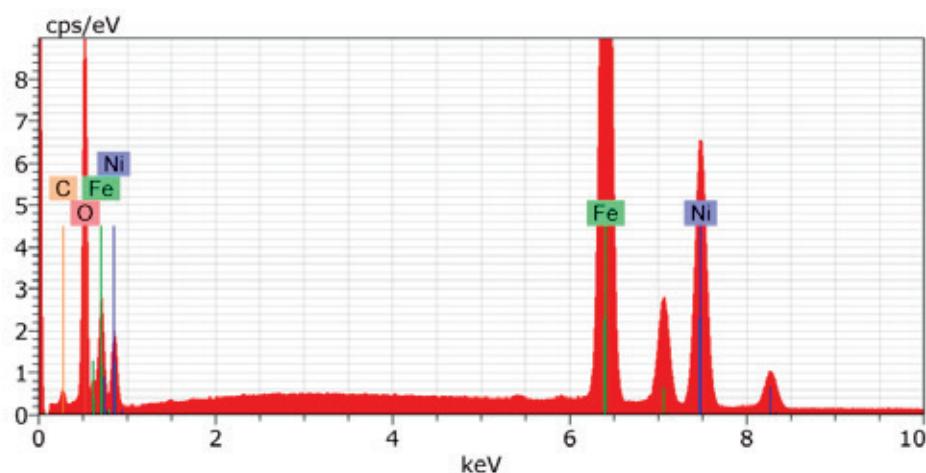


Fig. 3. Energy dispersive spectrum of  $\text{NiFe}_2\text{O}_4$

Table 1. Results of energy dispersion analysis of ferrite

Element	Weight %	Atomic %
O	30.50	55.05
Fe	40.19	20.78
Ni	24.21	11.91
C	5.10	12.26

crystallites had a pronounced agglomeration (Fig. 4). TEM data allows assuming that  $\text{NiFe}_2\text{O}_4$  agglomerates up to  $20\ \mu\text{m}$  in size were formed by nanoparticles below  $100\ \text{nm}$  in size. In the SEM image, equiaxial small particles with pronounced crystallinity clearly differentiated.

The rather high porosity of spinel is explained by the release of gaseous products of the polymer gel combustion, primarily carbon oxides  $\text{CO}$  and  $\text{CO}_2$ , which is a distinctive feature of nanoscale powders synthesized by citrate combustion [20].

It was experimentally established that nickel spinel nanopowder synthesized by citrate combustion is an effective heterogeneous catalyst for the hydrogen peroxide decomposition by a Fenton-like reaction. Oxidative degradation of MO under the influence of UV irradiation in the presence of the  $\text{NiFe}_2\text{O}_4$  catalyst proceeded more intensely than in its absence (Fig. 5). Therefore, the concentration of the dye during catalytic oxidation 2.5 hours after the beginning of the reaction decreased by 17 times. In the absence of a catalyst, after 2.5 hours of the reaction, the concentration of MO decreased only by 2 times.

The degree of degradation of the methylene orange dye without catalyst in visible light

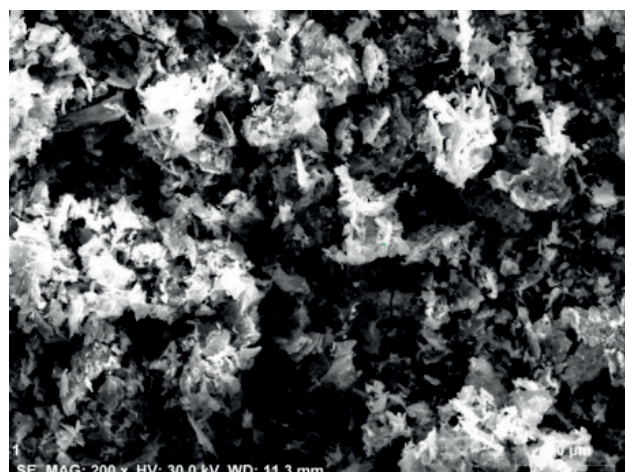
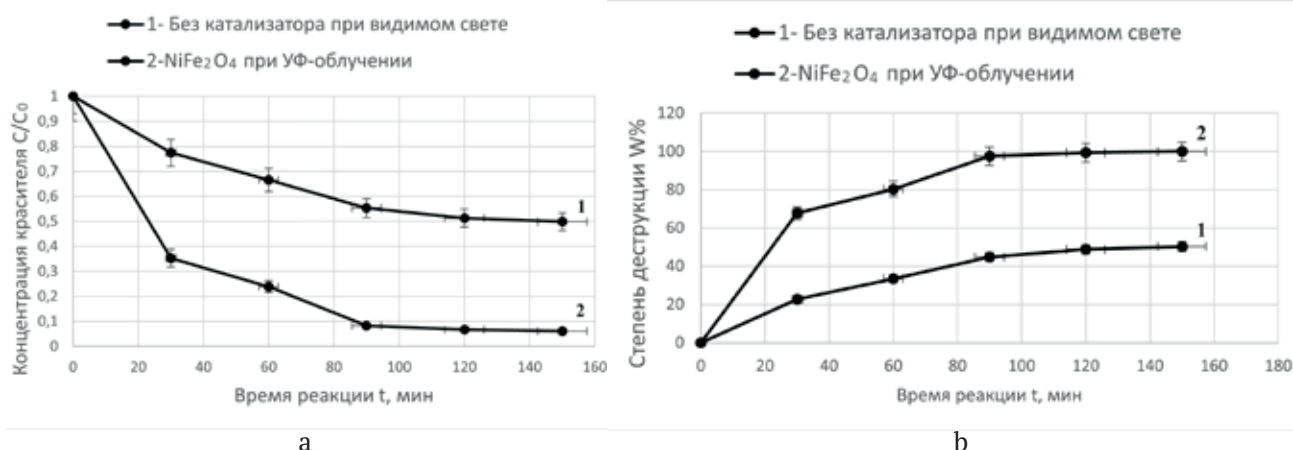


Fig. 4. SEM image of  $\text{NiFe}_2\text{O}_4$  nanopowder

2.5 hours after the beginning of the reaction was 50%. In the presence of nickel (II) ferrite under UV irradiation of the reaction mixture, the degree of degradation of MO increased to 99%.

The shape of kinetic curves of the oxidative degradation of the dye corresponded to the pseudo-first order of the reaction. The rate constant was evaluated by linearization of the kinetic dependences in logarithmic coordinates (Fig. 6). The rate constant of oxidative degradation of MO under UV irradiation in the presence of  $\text{NiFe}_2\text{O}_4$  was  $0.0191\ \text{min}^{-1}$ . The rate constant in the absence of a catalyst with natural lighting was almost an order of magnitude lower ( $0.0044\ \text{min}^{-1}$ ).

The process without the  $\text{H}_2\text{O}_2$  oxidant revealed a small sorption capacity of nickel spinel towards MO, the concentration of the dye decreased by



**Fig. 5.** Change in the concentration (a) and degree of degradation (b) of the MO dye without catalyst (1) and in the presence of NiFe<sub>2</sub>O<sub>4</sub> under UV irradiation (2)

7.5% 2.5 hours after the beginning of the reaction (Fig. 7).

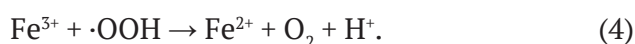
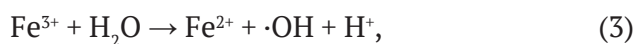
The sorption capacity of NiFe<sub>2</sub>O<sub>4</sub> reached its maximum value of 0.132 mg/g in 120 min (Fig. 7, insert), which indicates a slight contribution of sorption to the overall process of decolorization of the MO solution in the presence of a nanoscale NiFe<sub>2</sub>O<sub>4</sub> catalyst.

The structure of the mixed spinel, characteristic of nickel (II) ferrite means that Fe<sup>3+</sup> ions distribute in octahedral and tetrahedral voids. The catalytic activity of spinel ferrites in Fenton processes is due to the formation of active oxidants with their participation during the decomposition of hydrogen peroxide. According to [21], the formation of ·OH hydroxyl radicals is associated with the activity of Fe<sup>2+</sup> ions, whereas Fe<sup>3+</sup> ions are mainly responsible for the formation of ·OOH radicals. The oxidation state

for octahedral ions of Fe<sup>3+</sup> changes to +2 due to lattice oxygen [22]. Fe<sup>3+</sup> ions in the tetrahedral position exhibit electron-withdrawing properties (reaction 1) and contribute to the formation of active sites of the Fenton-like reaction of Fe<sup>2+</sup>, on which the decomposition of hydrogen peroxide is accompanied by the formation of hydroxyl radicals (reaction 2):



UV irradiation induces regeneration of Fe<sup>2+</sup> accompanied by the formation of hydroxyl radicals and molecular oxygen (reactions 3, 4):



The oxidizing radicals oxidize the dye molecule according to equation (5):

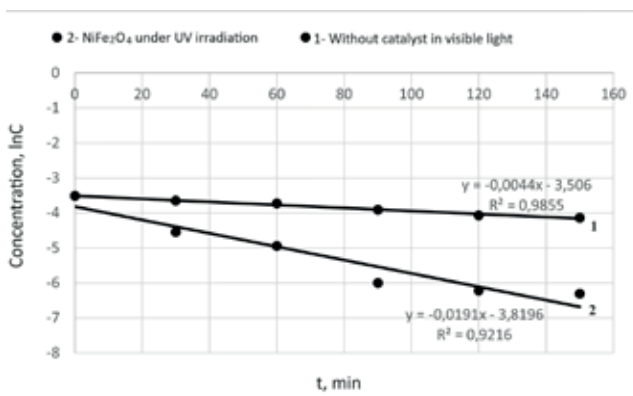


**Fig. 6.** Kinetic curves of MO oxidation by hydrogen peroxide in lnC - t coordinates without catalyst (1) and in the presence of NiFe<sub>2</sub>O<sub>4</sub> catalyst (2)

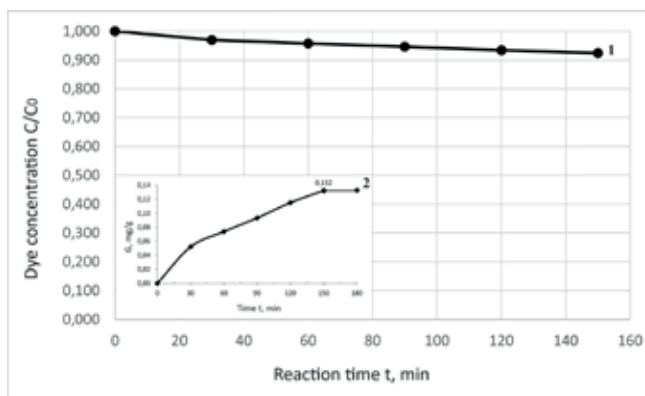
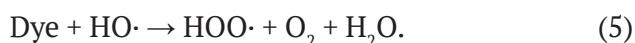


**Fig. 7.** MO sorption curves in the presence of NiFe<sub>2</sub>O<sub>4</sub> (1) and sample sorption capacity (2)



Previously, under similar conditions we established a rate constant of  $0.0354 \text{ min}^{-1}$  for nanoscale  $\text{CoFe}_2\text{O}_4$  with a reverse spinel structure as a catalyst of Fenton-like reaction of methyl orange oxidation [23]. Probably, the  $\text{Co}^{2+}/\text{Co}^{3+}$  pair in the spinel lattice increases the catalytic activity of cobalt ferrite as compared to  $\text{NiFe}_2\text{O}_4$  due to accelerated electron transfer.  $\text{Co}^{2+}$  cobalt ions are located in the center of the oxygen octahedra, and electrons of oxygen ions can easily participate in the oxidation of  $\text{H}_2\text{O}_2$  accompanied by the formation of hydroxyl radicals and the change of the oxidation state of cobalt to +3. The probability of participation of nickel ions due to the predominant oxidation state of +2 in such a process is much lower, however, in [24], X-ray photoelectron spectroscopy was used to confirm the presence of  $\text{Ni}^{3+}$  ions in nickel spinel after ozone treatment of oxalic acid. However, it should be emphasized that the value of the rate constant of MO oxidation in the presence of  $\text{NiFe}_2\text{O}_4$  exceeded the value for the oxidative degradation of MO under similar conditions when nanoscale normal spinel  $\text{ZnFe}_2\text{O}_4$  was present as a catalyst ( $0.010 \text{ min}^{-1}$ ), where A cation also had one oxidation state +2 despite a sufficiently high specific surface area of the catalyst ( $453.1 \text{ m}^2/\text{g}$ ) [25]. This is consistent with the data in [24] about poor capability of  $\text{ZnFe}_2\text{O}_4$  to transfer electrons when A cation changes to the  $\text{Zn}^{3+}$  state.

## Conclusions

Citrate combustion was used to synthesize a nanoscale nickel ferrite with a spinel structure (XRD data) with an average particle size of  $38 \pm 3 \text{ nm}$  (TEM data). It was established that nanodispersed  $\text{NiFe}_2\text{O}_4$  had high catalytic activity in the Fenton-like reaction of methyl orange dye oxidation. Under optimized conditions and effective control of parameters, including contact time, solution pH, and catalyst dose and under additional UV irradiation, over 99% of the pollutant was removed. The oxidative degradation of the dye without catalyst was 50%. The rate constant of oxidative degradation of MO under UV irradiation in the presence of nickel (II) ferrite was  $0.0191 \text{ min}^{-1}$ , while in the absence of a catalyst and in natural lighting it was  $0.0044 \text{ min}^{-1}$ . The sorption capacity of

$\text{NiFe}_2\text{O}_4$  reached its maximum value of  $0.132 \text{ mg/g}$  120 min after the beginning of the reaction, which means that the contribution of sorption to the decolorization of the MO solution is insignificant.

## Author contributions

All authors made an equivalent contribution to the preparation of the publication.

## Conflict of interests

The authors declare that they have no known competing financial interests or personal relationships that could have influenced the work reported in this paper.

## References

1. Gagan K. B., Sumit B., Mahavir S., Khalid M. B. *Ferrites and multiferroics fundamentals to applications: fundamentals to applications*. Springer Singapore; 2021. 213 p. <https://doi.org/10.1007/978-981-16-7454-9>
2. Sharma S. K. (ed). *Spinel nano ferrites. Synthesis, properties and applications*. Springer Cham; 2021. 475 p. <https://doi.org/10.1007/978-3-030-79960-1>
3. Winiarska K., Klimkiewicz R., Tylus W., ... Szczygieł I. Study of the catalytic activity and surface properties of manganese-zinc ferrite prepared from used batteries. *Journal of Chemistry*. 2019;201: 1–14. <https://doi.org/10.1155/2019/5430904>
4. Ramazania A., Fardood S. T., Hosseinzadeha Z., ... Jooc S. W. Green synthesis of magnetic copper ferrite nanoparticles using tragacanth gum as a biotemplate and their catalytic activity for the oxidation of alcohols. *Iranian Journal of Catalysis*. 2017;7(3): 181–185.
5. Taghavi Fardood S., Ramazani A., Golfar Z., Joo S. W. Green synthesis of  $\alpha\text{-Fe}_2\text{O}_3$  (hematite) nanoparticles using tragacanth gel. *Quarterly Journal of Applied Chemical Research*. 2017;11(3): 19–27.
6. Thomas J., Thomas N., Girgsdies F., Beherns M., Huang X., Sudheesh V. D. Synthesis of cobalt ferrite nanoparticles by constant pH co-precipitation and their high catalytic activity in CO oxidation. *New Journal of Chemistry*. 2017;41: 7356–736. <https://doi.org/10.1039/C7NJ00558J>
7. Zelenskaya E. A., Chernyshev V. M., Shabelskaya N. P., Sulima S. I., Sulima E. V., Semchenko V. V., ... Vlasenko A. I. Study of catalytic activity of oxides of transition elements in the reaction of hydrogen peroxide decomposition. *Fundamentalnye issledovaniya = Fundamental studies*. 2016;4: 261–265. (In Russ).
8. Artemyanov A. P., Zemsikova L. A., Ivanov V. V. Catalytic liquid-phase oxidation of phenol in water media using carbon fiber (iron, iron oxide) catalyst. *Izvestia vysshikh uchebnykh zavedenii Khimiya Khimicheskaya Tekhnologiya = News of higher education institutions. Series: Chemistry and Chemical Technology*.

2017;60(8): 88–95. (In Russ). <https://doi.org/10.6060/tcct.2017608.5582>

9. Ding C., Zhao H., Zhu X., Liu X. Preparation of cotton linters' aerogel-based C/NiFe<sub>2</sub>O<sub>4</sub> photocatalyst for efficient degradation of methylene blue. *Nanomaterials*. 2022;12(12): 2021. <https://doi.org/10.3390/nano12122021>

10. Goma H., Abd El-Monaem E. M., Eltaweil A. S., Omer A. M. Efficient removal of noxious methylene blue and crystal violet dyes at neutral conditions by reusable montmorillonite/NiFe<sub>2</sub>O<sub>4</sub>@amine-functionalized chitosan composite. *Scientific Reports*. 2022;15;12(1): 15499. <https://doi.org/10.1038/s41598-022-19570-1>

11. Tomina E., Novikova L., Kotova A., ... Alekhina Y. ZnFe<sub>2</sub>O<sub>4</sub>/zeolite nanocomposites for sorption extraction of Cu<sup>2+</sup> from aqueous medium. *Applied Chem*. 2023;(3):452–476. <https://doi.org/10.3390/applied-chem3040029>

12. Rashidi S., Ataie A. One-step synthesis of CoFe<sub>2</sub>O<sub>4</sub> nano-particles by mechanical alloying. *Advanced Materials Research*. 2014;829: 747–751. <https://doi.org/10.4028/www.scientific.net/amr.829.747>

13. Srinivasa Rao K., Ranga Nayakulu S. V., Chaitanya Varma M., Choudary G. S. V. R. K., Rao K. H. Controlled phase evolution and the occurrence of single domain Co<sub>x</sub>Fe<sub>2-x</sub>O<sub>4</sub> nanoparticles synthesized by PVA assisted sol-gel method. *Journal of Magnetism and Magnetic Materials*. 2018;451(1): 602–608. <https://doi.org/10.1016/j.jmmm.2017.11.069>

14. Manikandan A., Sridhar R., Arul Antony S., Ramakrishna S. A simple aloe vera plant-extracted microwave and conventional combustion synthesis: morphological, optical, magnetic and catalytic properties of CoFe<sub>2</sub>O<sub>4</sub> nanostructures. *Journal of Molecular Structure*. 2014;1076: 188–200. <https://doi.org/10.1016/j.molstruc.2014.07.054>

15. Petrova E., Kotsikau D., Pankov V., Fahmi A. Influence of synthesis methods on structural and magnetic characteristics of Mg–Zn-ferrite nanopowders. *Journal of Magnetism and Magnetic Materials*. 2019;473: 85–91. <https://doi.org/10.1016/j.jmmm.2018.09.128>

16. Mittova I. Ya., Tomina E. V., Lavrushina S. S. *Nanomaterials: synthesis of nanocrystalline powders and production of compact nanocrystalline materials\**. Textbook for universities. Voronezh: Publisher: IPC VSU Publ.; 2007. (In Russ.)

17. Meshcheryakova A. A., Tomina E. V., Titov S. A. Study of the sorption and catalytic properties of nickel ferrite with respect to 2,4-dinitrophenol. *High Energy Chemistry*. 2023;57: 342–345. <https://doi.org/10.1134/S0018143923080180>

18. JCPDC PCPDFWIN: A Windows Retrieval/Display program for Accessing the ICDD PDF – 2 Data base. International Centre for Diffraction Data, 1997.

19. Brandon D., Kaplan U. *Microstructure of materials. Research and control methods*. West Sussex: John Wiley & Sons Ltd; 1999, p. 384.

20. Tomina E. V., Kurkin N. A., Konkina D. A. ZnFe<sub>2</sub>O<sub>4</sub> nanoscale catalyst for wastewater treatment from dyes by oxidative degradation. *Ecology and Industry of Russia*. 2022;26(5): 17–21. (In Russ). <https://doi.org/10.18412/1816-0395-2022-5-17-21>.

21. Maldonado A. C. M., Winkler E. L., Raineri M., ... Lima E. Free-radical formation by the peroxidase-like catalytic activity of MFe<sub>2</sub>O<sub>4</sub> (M = Fe, Ni, and Mn) nanoparticles. *The Journal of Physical Chemistry C*. 2019;123(33): 20617–20627. <https://doi.org/10.1021/acs.jpcc.9b05371>

22. Tatarchuk T., Shyichuk A., Trawczyńska I., ... Gargula R. Spinel cobalt(II) ferrite-chromites as catalysts for H<sub>2</sub>O<sub>2</sub> decomposition: synthesis, morphology, cation distribution and antistructure model of active centers formation. *Ceramics International*. 2020;46(17): 27517–27530. <https://doi.org/10.1016/j.ceramint.2020.07.243>

23. Kurkin N. A., Volkov A. S., Doroshenko A. V., Gudkova N. A., Tomina E. V. *Actual problems of theory and practice of heterogeneous catalysts and adsorbents: Proceedings of the VII All-Russian scientific conference\**. Kazan; 2023. pp. 248–249. (In Russ.)

24. Zhang F., Wu C., Kaiyi W., Zhou H., ... Wei S. Ozonation of aqueous phenol catalyzed by biochar produced from sludge obtained in the treatment of coking wastewater. *Journal of Environmental Management*. 2017;547: 60–68. <https://doi.org/10.1016/j.jenvman.2018.07.038>

25. Shabelskaya N. P., Egorova M. A., Vasileva E. V., Polozhentsev O. E. Photocatalytic properties of nanosized zinc ferrite and zinc chromite. *Advances in Natural Sciences: Nanoscience and Nanotechnology*. 2021;12(1): 015004. <https://doi.org/10.1088/2043-6254/abde3b>

\*Translated by author of the article

### Information about the authors

*Anna A. Meshcheryakova*, postgraduate student at the Department of Materials Science and Industry of Nanosystems, Voronezh State University, (Voronezh, Russian Federation).

<https://orcid.org/0000-0003-4899-609X>  
anna-meshcheryakova@internet.ru

*Elena V. Tomina*, Dr. Sci. (Chem.), Head of the Department of Chemistry, Voronezh State University of Forestry and Technologies named after G. F. Morozov (Voronezh, Russian Federation).

<https://orcid.org/0000-0002-5222-0756>  
tomina-e-v@yandex.ru

*Anh Tien Nguyen*, PhD (Chem.), Associate Professor, Head of the Inorganic Chemistry Department, Ho Chi Minh City University of Education Vietnam (Ho Chi Minh City, Vietnam).

<https://orcid.org/0000-0003-3919-8571>  
tienna@hcmue.edu.vn

*Alexander I. Dmitrenkov*, Cand. Sci. (Tech.), Associate Professor, Voronezh State Forestry University named after G. F. Morozov (Voronezh, Russian Federation).

<https://orcid.org/0000-0001-9296-1762>  
dmitrenkov2109@mail.ru

*Received 26.03.2024; approved after reviewing 22.04.2024; accepted for publication 15.05.2024; published online 01.10.2024.*

*Translated by Irina Charychanskaya*